MSD SIMULATION IN LAP JOINTS USING A DBEM MODEL

GARCIA A N*, IRVING P E*
*SIMS, CRANFIELD UNIVERSITY, CRANFIELD, BEDS MK43 0AL, UK

Keywords: *AGING AIRCRAFT, MSD, LAP JOINT, DBEM*

Abstract

Multiple Site Damage (MSD) is characterized by the development of simultaneous fatigue cracks at multiple sites in the same structural element. Among all aeronautical structures prone to develop MSD, riveted lap-splice joints in the fuselage have been identified as being the most susceptible. In this work a complete MSD assessment based on Monte Carlo (MC) simulation has been conducted for a typical aircraft three-row unstiffened lap-splice joint configuration. Based on the Dual Boundary Element Method (DBEM), a simple model for representing cracked lap joints has been presented and a geometrical correction factor (β) study conducted. The results demonstrated that β values can be influenced by cracks positioned more than one pitch distance away from one another. Secondly, a probabilistic model for MSD assessment considering both fatigue crack initiation and crack propagation as random variables has been presented. The results obtained from the MSD assessment model provided good agreement with published experimental work on fatigue of lap splice joints. It was observed that a great number of the scenarios generated by Monte Carlo simulation contained only one crack, and therefore they can not represent MSD-like situations. Invariably part of the whole Monte Carlo simulation failure process was dominated by propagation of only a few large cracks, resulting in longer lives than the ones found in 'true' MSD situations. Finally, a possible change of the standard deviation value for the initiation of fatigue cracks was investigated in the MSD assessment model. The results indicated that the number of MSD-like scenarios and the mean time to initiation and to propagation of fatigue cracks was modified. As a consequence of this observation, it is clear that both the Inspection Starting Point (ISP) and the Structural Modification Point (SMP) must be defined with care. These issues are critically assessed in this paper.

1 Introduction

Multiple Site Damage (MSD) is characterized by the development of simultaneous fatigue cracks at multiple sites in the same structural element. Among all aeronautical structures prone to develop MSD, riveted lap-splice joints in the fuselage have been identified as being the most susceptible [1]. When MSD cracks are present, crack propagation time decreases rapidly and the residual strength of the structural element is degraded. To investigate this failure mode, in this work a complete MSD assessment based on Monte Carlo (MC) simulation has been conducted for a typical aircraft three-row unstiffened lap-splice joint configuration.

Recent recommendations by regulators [1] to avoid MSD threat stipulate an inspection starting point and a structural modification point in the service life of aircraft. These points can be defined in terms of MSD analysis results, test results and/or by service experience. The intention is that the aircraft shall not be operated while there is a significant probability that MSD is present. Capability to accurately calculate service life to MSD onset becomes of considerable importance.

Previous workers have approached MSD by considering the probabilistic nature of its

occurrence, and have employed Monte Carlo techniques to simulate the stochastic nature of fatigue crack initiation at fastener holes and /or subsequent crack propagation, and therefore calculate the distribution of lives to MSD onset, link-up and ultimate failure.

The crack initiation stage is commonly addressed by applying Monte Carlo simulation to lognormal or Weibull distributions of lives to achieve a specified crack size a_o [1]. The following crack propagation stage is simulated either deterministically or probabilistically.

There are particular difficulties in calculation of stress intensities for crack growth in MSD crack configurations because the β correction term will change for every different crack configuration simulated. Therefore the technique used for stress intensity calculation must be accurate and economical of computer time if it is to be used in a repeated simulation such as the Monte Carlo. In previous work, finite elements [2], alternating finite elements [3], boundary elements [4], dual boundary elements [5] and compounding method [6] have all been used to calculate stress intensities of MSD cracks. The DBEM previously demonstrated that the high stress gradients near the crack tips can be modelled more accurately and efficiently than domain methods, such as Finite Elements (FE), and it is able to analyse multiple cracks in complex geometrical configurations [7]. A typical MSD situation consists of a row of pin-loaded holes with a large number of edge and embedded cracks under mixed mode loading conditions. The most attractive feature of the DBEM is the reduction of the dimensionality of the numerical model, when compared to FE. Crack problems can be analysed and Stress Intensity Factor (SIF) values determined without any re-meshing being required. Therefore the DBEM approach is better suited than FE for multiple crack growth scenarios generated by Monte Carlo (MC) simulations.

Previous MSD simulations using DBE have used deterministic crack growth together with open hole geometries in their analysis [5]. In this work the DBE formulation [7, 8] has been applied to a row of pin loaded holes to perform probabilistic crack growth simulation of MSD using the Monte Carlo approach.

In the next sections of this work, the accuracy of a simple idealized DBE lap joint model is established by comparison with published FE stress intensity data. Secondly, a case study of geometrical correction factor (β) is undertaken to establish and to understand the role of multiple crack interactions on β values. Finally, a methodology for MSD assessment is presented and a typical riveted lap joint, consisting of 3 rows of 9 holes, is employed to establish the ISP and the SMP and the results critically assessed.

2 Lap Joint Modelling

In order to represent MSD behaviour in lap joints, the first step that has to be taken into to account is the effectiveness of the model used to obtain fundamental parameters such as the stress intensity factor values. Regarding this issue, a simple lap joint model based on the DBEM is described in this section, and the values obtained for the Stress Intensity Factor (SIF) are compared to the ones obtained from the literature [9].

The lap joint geometry selected to be modelled is the one presented in Fig. 1 and it has been analysed by Cope [9] by means of FE modelling. The lap joint is subjected to a remote tensile stress of S_0 = 68.96 MPa and is constructed of two W = 609.6 mm wide 2024-T3 aluminium panels (t = 1.6 mm) fastened together with steel rivets (ϕ = 4.76 mm). The pitch distance (p), row spacing (s) and edge distance (e) are 25.4 mm, 25.4 mm and 12.7 mm, respectively. A 203.2 mm slot connected the nine centre fasteners in the upper row, and a lead crack is introduced at each of the outer two fasteners of the slot. MSD cracks are introduced at adjacent fastener holes to the lead crack tips.

The DBEM formulation utilized here for the stress intensity calculation developed by Salgado [7, 8] has been incorporated in the DTD code [10], which is used in this work for analysing a cracked lap joint configuration. The lap joint model idealized with the DTD Code is illustrated in Fig. 2, and it consists of one

rectangular sheet of aluminium 2024 T-3, 609.6 mm long and 304.8 mm wide, discretized by 94 boundary elements and 188 nodes, with a lead crack and two MSD cracks represented by the numbers 3, 2 and 1, respectively; with a central row of seven pin-loaded holes (representing the upper row of holes of the lap joint illustrated in Fig. 1), left constraint (D_x) in the x direction to simulate symmetry and a lateral constraint (D_y) in the y direction where no displacements are expected. The hole diameter, pitch distance, edge distance and sheet thickness are the same as illustrated in Fig. 1. The concept of load transfer is used and the values of stresses applied in the model are the remote tensile stress S_0 = 68.96 MPa in the top of Fig. 2 and the bypass stress S_{bp} = 56.88 MPa in the bottom of Fig 2; both of them represented by the T_y traction vectors. The value of S_{bp} is obtained considering that the holes traversed by the lead crack do not react to the remote stress S_0 and therefore these loads are globally redistributed together with the ones from the middle and bottom rivet reaction loads as illustrated in Fig. 1.

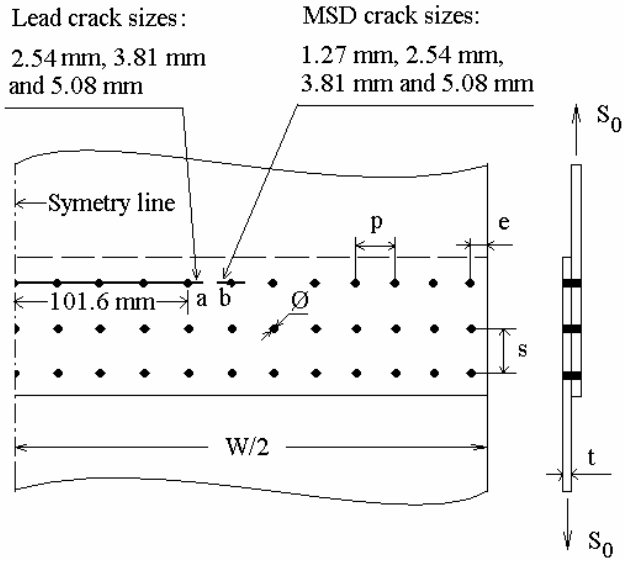

Fig. 1. Fastened lap joint.

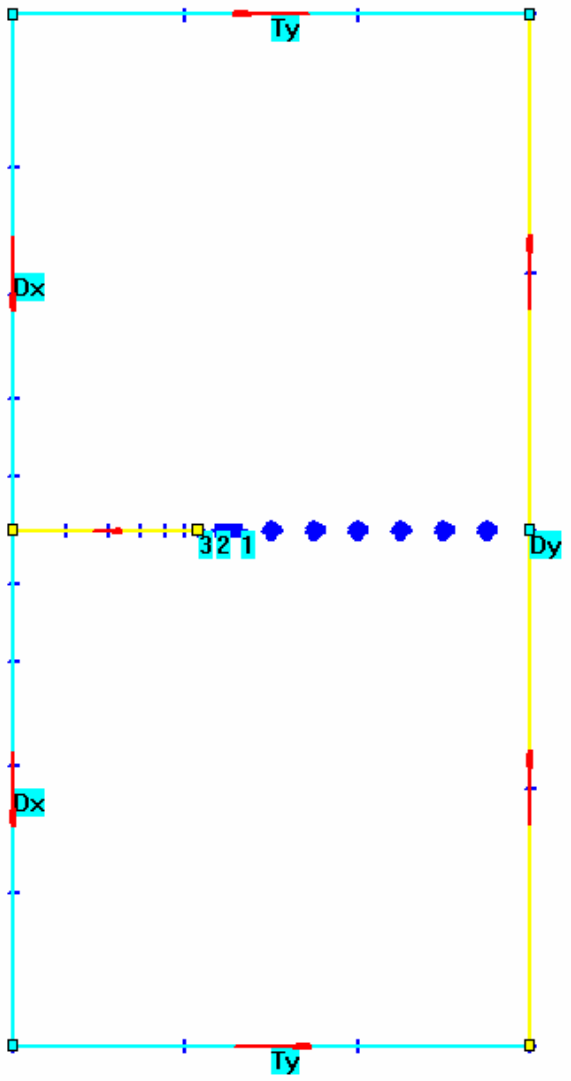

Fig. 2. DBE model for Fig. 1 lap joint.

The model shown in Fig. 2 is then run by the DTD code [10], and the results of the SIF values for the lead crack 'a' (Fig. 1) $K_{Ia\text{-}dtd}$ (from this work) and $K_{Ia\text{-}ref.}$ (from Reference [9]) are presented in Table 1. It can be seen that the differences (E) between both models ranged from – 2.22 % to – 1.19 %, with an average error of – 1.84 %. The SIF values for the MSD crack 'b' (Fig. 1) $K_{Ib\text{-}dtd}$ (from this work) and $K_{Ib\text{-}ref.}$ (from Reference [9]) are presented in Table 2. From Table 2, the differences (E) between both models ranged from +0.82 % to -3.32 %, with an average error of – 1.54 %.

Table 1: Comparison of SIF for the lead crack

a_{lead} (mm)	a_{msd} (mm)	$K_{Ia\ -\ dtd}$ ($MPa\sqrt{mm}$)	$K_{Ia\ -\ ref.}$ ($MPa\sqrt{mm}$)	E (%)
2.54	-	1377	1400	-1.64
2.54	1.27	1380	1406	-1.85
2.54	2.54	1394	1417	-1.68
3.81	-	1387	1415	-1.98
3.81	1.27	1390	1421	-2.22
3.81	2.54	1406	1435	-2.06
3.81	3.81	1433	1454	-1.19
5.08	-	1402	1427	-1.75
5.08	1.27	1406	1434	-2.01
5.08	2.54	1429	1450	-1.48
5.08	3.81	1440	1472	-2.22
5.08	5.08	1472	1502	-2.01

Table 2: Comparison of SIF for the MSD crack

a_{lead} (mm)	a_{msd} (mm)	$K_{Ia\ -\ dtd}$ ($MPa\sqrt{mm}$)	$K_{Ia\ -\ ref.}$ ($MPa\sqrt{mm}$)	E (%)
2.54	1.27	499.0	494.8	0.82
2.54	2.54	592.5	605.7	-1.69
3.81	1.27	511.9	510.8	0.17
3.81	2.54	608.8	623.7	-2.42
3.81	3.81	702.9	716.2	-1.88
5.08	1.27	534.2	528.5	-1.04
5.08	2.54	637.2	648.4	-1.76
5.08	3.81	722.5	747.1	-3.32
5.08	5.08	821.2	844.4	-2.77

These results comparison demonstrate a good level of agreement for the whole range of lead and MSD crack sizes, despite the differences inherent to both models (see Reference [9]). The simple lap joint model idealized in Fig. 2 shows its effectiveness when it comes to analysing a complex lap joint configuration such as the one illustrated in Fig. 1; and therefore this type of model will be used in the present paper for calculation of SIF values.

3 Geometrical Correction Factor Case Study

A comprehensive study of the geometrical correction factor (β), for a wide range of crack configurations, was undertaken to establish and to understand the role of multiple crack interactions on stress intensity factors [11]. In the current section, part of the results obtained in Reference [11] is presented here. These results are concerned to the investigation of how equal-sized cracks can influence each others' geometrical correction factors. To perform this task, the lap joint geometry selected to be analysed is shown in Fig. 3 and consists of 3 rows of 9 pin-loaded holes. It is subjected to a uniform remote alternating tensile stress with maximum stress of S_0 = 100 MPa and an R ratio (min stress/max stress) of 0.1. The sheet is 1.6 mm thick and is of clad 2024 T3. The rivet diameter (ϕ) is 4 mm, and the pitch distance (p), the inter row spacing (s) and the edge distance (e) are all equal to 20 mm. The ultimate tensile strength, proof strength and fracture toughness are 448 MPa, 331 MPa and 32 MPa $m^{1/2}$, respectively.

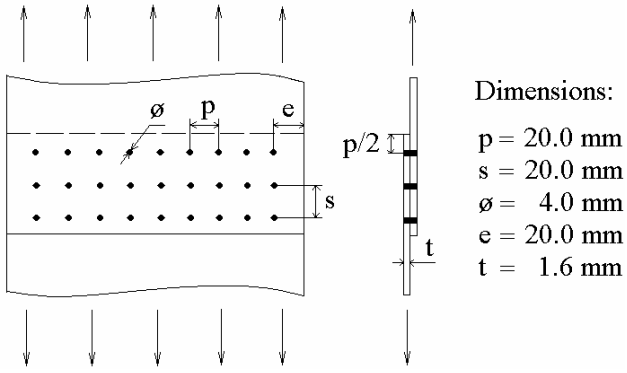

Fig. 3. Lap joint configuration

As is section 2, the same procedure for the idealization of the DBEM model is adopted for modelling the lap joint illustrated in Fig. 3. It consists of one rectangular sheet, 464 mm long and 200 mm wide, discretized by 164 boundary elements and 328 nodes, with a central row of nine pin-loaded holes (representing the upper row of holes of the lap joint illustrated in Fig. 3) and lateral constraints (D_x) in the x direction to

simulate a wider joint. The hole diameter, pitch distance, edge distance and sheet thickness are the same as illustrated in Fig. 3. The concept of load transfer is used and the values of stresses applied in the model are the remote tensile stress S_0 = 100 MPa and the bypass stress S_{bp} = 64.5 MPa in the bottom. The value of S_{bp} is obtained from the rivet reaction loads from the middle and bottom rows illustrated in Fig. 3.

Fig. 4 illustrates the convention adopted for possible positions of crack tips in the upper row of the 3x9 rivets lap joint from Fig. 3. For example, when crack tips a1 and a2 are present, this means that there are two crack tips placed in positions 1 and 2 according to the convention adopted.

In all cases presented in this section, the geometrical correction factors (β) are represented by the following non-dimensional ratio,

$$\beta = K_I/K_0 \qquad (1)$$

Where K_I is the mode I stress intensity factor, $K_0 = S_0\sqrt{\pi a_1}$, S_0= 100 MPa is the remote applied stress and a_1 is the crack length.

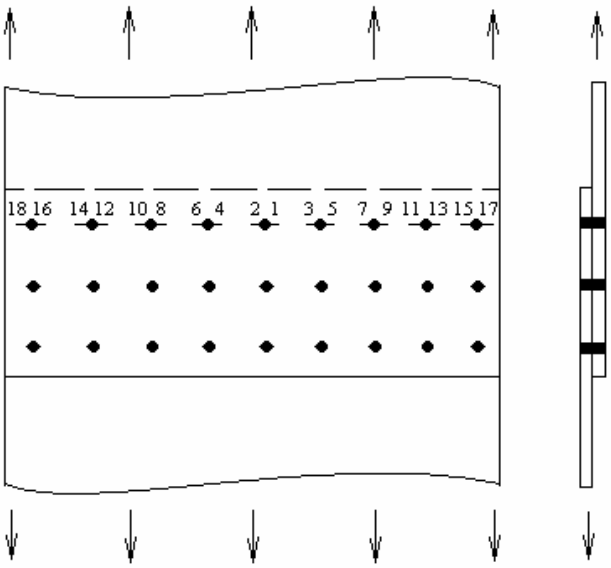

Fig. 4. Convention for crack tip positions.

Fig. 5 compares the geometrical correction factors for crack tip 1, considering the cases of one crack (placed in position 1) and two cracks (placed in positions 1 and 4, 1 and 8, 1 and 12). For (a_1/p) = 0.70, it can be noted that β for one crack (position 1) and two cracks (position 1 and 4) increases by 13.3 %. For one crack (position 1) and two cracks (positions 1 and 8) the difference is 2.4 %. For one crack (position 1) and two cracks (positions 1 and 12) the difference is 1.2 %. When comparing crack tips 1 and 4 to the other cases, it can be seen that differences in the β values start to become noticeable from (a/p) = 0.25. These results suggest that when a crack exists in position 1, the influence that a second crack placed in positions 8, 12 or 16 is less than 2.5 % and it could be neglected with respect to crack tip 1.

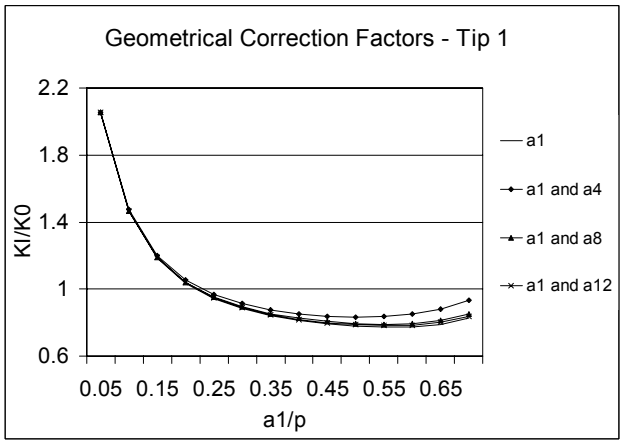

Fig. 5. Geometrical correction factors comparison for the case of single cracks.

Fig. 6 compares the geometrical correction factors for crack tip 1, considering two cracks (placed in positions 1 and 2) and four cracks (placed in positions 1, 2, 4 and 6; 1, 2, 8 and 10; 1, 2, 12 and 14; 1, 2, 16 and 18). For (a_1/p) = 0.70, it can be seen that β for two cracks (positions 1 and 2) and four cracks (positions 1, 2, 8 and 10) increases by 11.3 %. For two cracks (positions 1 and 2) and four cracks (positions 1, 2, 12 and 14) the difference is 5.2 %. For two cracks (positions 1 and 2) and four cracks (positions 1, 2, 16 and 18) the difference is 3.5 %. For the lap joint illustrated

in Fig. 4, the unique β value difference less than to 5 % is the case of the central cracked hole and the left extreme cracked one. For crack tips '1, 2, 8 and 10' and '1, 2, 12 and 14' cases, the β values will differ more than 5 % for, respectively, a range of (a/p) ratios starting from 0.50 to 0.70 (see Reference [9]).

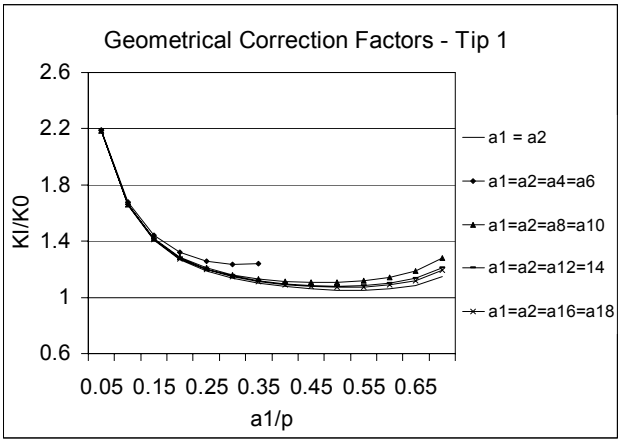

Fig. 6. Geometrical correction factors comparison for the case of double cracks.

From the results presented in Fig. 5 and Fig. 6, it can be concluded that although adjacent cracked holes play the most important role on crack interaction effects; for a range of (a/p) ratios, crack interaction can also take place in cracked holes separated by two, three or four pitch distances, depending on the cracked scenario analysed. Any geometrical correction factors evaluation for MSD assessment shall be able to analyse such cases to correctly represent crack interaction. The use of computer codes that are able to cope with any possible damage scenario generated by Monte Carlo simulations, such as the DTD code [10], seems to be the adequate choice. In the next sections, the DTD code [10] is employed to perform multiple crack growth according to the proposed methodology for MSD assessment.

4 MSD Assessment Approach

Regarding MSD assessment of a lap joint in a frame-bay, models reported in the literature consist of only 8 to 10 pin-loaded holes. The reason for the small number of holes is well summarized by Horst [12] where he notes that in stiffened lap joints a nearly quadratic stress distribution is found within one frame-bay and the maximum of this distribution is located in the centre of the bay. Therefore 8 to 10 rivets are loaded in such a manner that the fatigue life can be very similar compared to the one in the centre of the bay. In fact, some tear down inspections performed in aging aircraft [13, 14] confirm that the crack pattern along a frame-bay lap joint is basically limited to the central holes which are within the highly stressed location. Bearing this in mind, the results presented in the next sections are representative of a typical lap joint configuration containing a row of 9 pin-loaded holes.

In this section, the MSD assessment model developed is presented in three separate parts: fatigue crack initiation, deterministic crack growth and probabilistic crack growth. The lap joint analysed is the one presented in Fig. 3 as described in section 3.

In the Monte Carlo simulation, the crack initiation stage and the crack propagation stage are considered separately. An initial analysis allocates initiated cracks of 1.5 mm at each fatigue critical location with a randomly selected life to achieve that crack length. This is followed by a LEFM based crack growth analysis. Final failure occurs either by exceedance of the material fracture toughness or net section yield. Details of each process are given in the following sections.

4.1 Fatigue Crack Initiation

To represent the fatigue crack initiation life 'N_0', a lognormal distribution of lives to achieve a crack size of 'a_0' is employed. Considering the external rows of a lap joint, it is assumed that each pin-loaded hole has two fatigue critical locations (FCL) at 3 and 9 o'clock positions of the hole border. For each FCL, the normal distribution '$\log(N_0)$' is defined by the mean S-N fatigue life 'μ', the standard deviation 'σ' and the standard normal distribution 'α' given by,

$$\log(N_0) = \mu + \alpha.\sigma \qquad (2)$$

When a random value of 'α' is generated by Monte Carlo simulation, one initial damage scenario is created by attributing each FCL a different initial fatigue life given by eqn (2). The S-N fatigue curve properties used for the riveted holes is from Santgerma [2], and the values for 'μ[log]' and 'σ[log]' are calculated as a mean value of, respectively, 5.6370 and 0.20 for an initial crack size a_o of 1.5 mm.

4.2 Crack Propagation

Crack tips emanating from pin loaded fastener holes are subjected to mixed mode stress fields, and the DBE program calculates both K_I and K_{II} components. A mixed mode stress intensity range ΔK_{eff} was calculated using the Tanaka [15] expression,

$$\Delta K_{eff} = \sqrt{\Delta K_I^2 + 2\Delta K_{II}^2} \qquad (3)$$

The Paris equation is used to calculate the crack growth rate (da/dN), given as a function of the effective stress intensity factor (ΔK_{eff}),

$$\frac{da}{dN} = C(\Delta K_{eff})^m \qquad (4)$$

Material constants C and m values are C = 6.09E-11, and m = 2.6, obtained from Salgado [10]. Crack growth lives are then calculated in the usual way using eqn (4), with a starting crack length a_o of 1.5 mm, the initiation crack size. As cracks grow, the Swift [16] criterion is used to define link-up. After link-up with an uncracked hole, continuing damage [17] is assumed (an initiated crack of length 0.127 mm is assumed to start from the opposite hole border to where link up took place). Final failure occurs when residual strength becomes inadequate on either material fracture toughness or net-section yield criteria.

4.3 Probabilistic Crack Growth

In order to represent the probabilistic nature of the fatigue crack growth, the Xing [18] formulation will be used to expand the Monte Carlo simulation applied to numerical techniques, such as the DBEM. Taking the logarithm on both sides of eqn (4) it follows,

$$\log\frac{da}{dN} = \log C + m\log\left(\Delta K_{eff}\right) \qquad (5)$$

To represent the stochastic nature of crack propagation, a normally distributed variable $Z \sim N(0, \sigma_z^2)$ is added to the logarithm of the fatigue crack growth law in eqn (5),

$$\log\frac{da}{dN} = \log C + m\log\left(\Delta K_{eff}\right) + Z \qquad (6)$$

Considering the properties of the standard normal distribution, the probability that a measurement will fall in a range $Z \le Z_p$ is given by $P(Z \le Z_p) = p$, and Z_p can be written as,

$$Z_p = \alpha_p \sigma_z \qquad (7)$$

When the probability 'p' is given, α_p can be obtained from the standard normal distribution. For example, when $p = 50\%$, $\alpha_p = 0$, leading $Z_p = 0$ in eqn (7), therefore eqn (6) becomes the deterministic average fatigue crack growth rate represented by eqn (5). The probabilistic crack growth rate, represented by eqn (6), can be simplified if the value of 'm' is assumed as a mean constant value and the probabilistic character of crack growth is attributed to the constant 'C', assumed as a lognormal distribution. Therefore, eqn (6) and (7) can be re-arranged as,

$$\log\left(\frac{da}{dN}\right)_p = \log C_p + m\log\left(\Delta K_{eff}\right) \qquad (8)$$

Where $\log C_p = \log C + \alpha_p \sigma_z$ is now a random variable normally distributed with mean $\log C$ and variance σ_z^2. Eqn (8) can be re-written as,

$$\frac{da}{dN} = [C \exp(\alpha_p \sigma_z)](\Delta K_{eff})^m \qquad (9)$$

For a given value of α_p, the number of cycles N_f to grow a crack from an initial crack size 'a$_0$' up to a crack size 'a$_f$' is obtained from direct integration of eqn (9),

$$N_f = \frac{1}{C \exp(\alpha_p \sigma_z)} \int_{a_0}^{a_f} \frac{da}{(\Delta K_{eff})^m} \qquad (10)$$

Based on Virkler's [19] findings, it is assumed here that each initial damage scenario has a unique α_p value. In this work $\sigma_z[\log] = 0.043$ has been assumed, following Proppe [3].

5 Results

5.1 MSD Assessment Approach Comparison

Regarding the MSD methodology proposed in section 4, the MSD assessment model is employed for analysing the lap joint configuration presented in Fig. 3 and the results compared to experimental work from the literature for validation of the approach. The results of 400 Monte Carlo simulations are presented in Fig. 7, together with 6 points from the test results of Foulquier [20]. In order to overcome the limited number of Monte Carlo simulations, confidence regions [21] are plotted to enclose a much wider range of possible outcomes. The confidence boundary limits have been corrected according to Arnold [22], so that a finite number of random simulations can produce the same confidence region size as an infinite number of simulations. Convergence of Monte Carlo simulations was checked for fatigue crack initiation and propagation lives, as well as the standard deviation outcome related to these lives. The necessity of checking for convergence relies on obtaining a minimum number of Monte Carlo simulations where the mean values of fatigue lives for initiation and propagation, as well as the related standard deviation values, reach stability around a mean value and it will not change significantly with increasing number of Monte Carlo simulations. When the stability is obtained, the mean values of fatigue lives for crack initiation and for crack propagation, as well as its standard deviations, can be used as unbiased estimators in order to plot dual confidence regions. In the case of this model for MSD assessment, a minimum number of 300 simulations is required.

As found in other published simulations, for instance Santgerma [2], Proppe [3] and Kebir [5], Fig. 7 shows that lives to failure are dominated by crack initiation, with mean initiation life equal to 180,000 cycles and the mean propagation life equal to 45,000 cycles, i.e., the initiation phase represents 80 % of the failure process. Total initiation life varies from 5.5×10^4 to 3.7×10^5 cycles, whereas propagation lives are between 1.5×10^4 to 7×10^4. Five of the six experimental points fall on or outside the 95% probability boundary line for the simulations, suggesting that real failure processes have considerably greater variability than the simulations. The mean propagation life of the experimental data is approximately the same as that of the simulations, but the spread of the 6 experimental propagation lives is as large as that of the entire 400 simulations. The spread of predicted lives encloses the range of scatter of the experimental lives for both initiation and propagation stages. However, there are only 6 experimental points; even for the 99.7 % confidence region there is one experimental point standing outside. It is likely that were 400 experiments to be performed, the observed scatter could be greater than the current data set.

From the results shown in Fig. 7, an interesting outcome observed is the one related to the number of cracks present in each single scenario generated by Monte Carlo simulation.

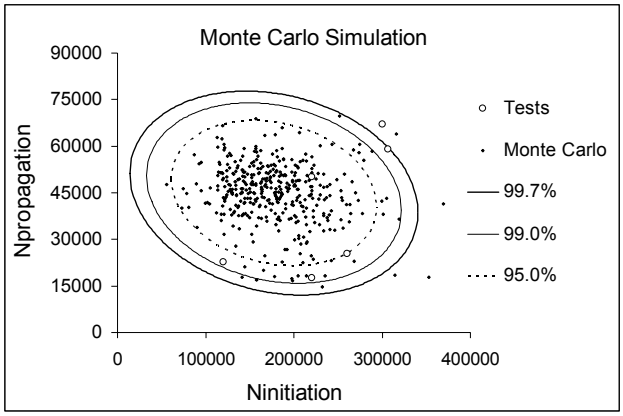

Fig. 7. Monte Carlo simulation results and its confidence boundaries in percentage

Fig. 8 shows the percentage of scenarios which developed 1, 2, 3 and 4 cracks. It can be seen that scenarios which developed only one crack represent 41 % of the cases generated by the Monte Carlo simulation presented in Fig. 7. These mono-crack scenarios do not represent what it could be expected as a MSD situation. Other workers [2] have obtained up to 60 % of mono-crack generated by Monte Carlo simulation.

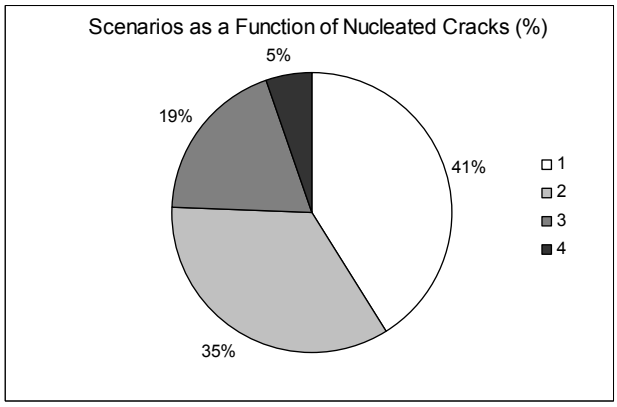

Fig. 8: Percentage of scenarios as a function of nucleated cracks for σ[log]= 0.20

Regarding the results presented in Fig. 8, a question related to the other 59 % of the scenarios that developed more than 1 crack could be placed: do these scenarios represent a MSD situation? According to Reference [1], 'MSD is a source of widespread fatigue damage characterized by the simultaneous presence of fatigue crack in the same structural element (i.e. fatigue cracks that may coalesce with or without other damage leading to a loss of required residual strength'. From this definition, it means that as far as more than one crack is present in the same structural element and they are long enough to coalesce with or without other damage (for example, other crack) causing the loss of residual strength then a MSD-like situation is present.

5.2 Effect of scatter in MSD assessment

In order to evaluate the effect of scatter (standard deviation) on the current MSD analysis, the scatter value for the initiation of fatigue cracks was changed and its consequences to MSD assessment results investigated. Scatter in crack initiation has been reported as one of the major factors to control the MSD phenomenon [23]. Rather than being a purely theoretical situation, different scatter values for approximately the same mean value of fatigue life for crack initiation is feasible to happen. For example, from Santgerma [2] the values for 'μ[log]' and 'σ[log]' are calculated as a mean values of, respectively, 5.6370 and 0.20; and therefore μ = 433,500 cycles for the geometry presented in Fig. 3. From Meyer [24], for 2024 aluminium alloys under constant amplitude testing mean values of σ[log] equal to 0.1486 is recommended. Current fatigue testing in the authors' laboratory are presently indicating that σ[log] equal to 0.09 should be used for μ values in a range of 200,000 cycles to 600, 000 cycles. The explanation for this great variability in σ[log] values is not the aim of this work, but it is possible that the manufacturing process quality makes a significant contribution.

While hand-riveted samples may exhibit large scatter values for initiation of fatigue cracks, because of non-homogeneity of hole size, the opposite situation can possibly be related to samples manufactured under tight control where holes are reamed to the desired diameter value, which gives a much proper expansion of the hole due to rivet interference

fit. The effect of proper hole expansion and its improvement to the mean fatigue life is reported by Swift [25], although the influence on the scatter itself would need further investigation. The main concern here is that for the same mean fatigue life, different σ[log] values can lead to different MSD results from Monte Carlo simulation, and this behaviour can influence the establishment of the ISP and the SMP.

Fig. 9 presents the mean value in cycles for initiation of the first fatigue crack as a function of different scatter values. As can be seen, the number of cycles for initiation of the first crack is extremely sensitive to changes in scatter, high scatter values lead to small number of cycles for fatigue crack initiation and the opposite situation is also true. For example, for standard deviations (log-scale) of 0.2 and 0.1 the mean values for initiation of the first crack (leading crack) increases from respectively, 180,000 cycles to 250,500 cycles.

In order to compare the differences that scatter produces in the whole MSD assessment, the same Monte Carlo simulation as presented in Fig. 7 is repeated here but with σ[log] equal to 0.09, which was chosen as a lower bound value. The results of 400 Monte Carlo simulations are presented in Fig. 10 and 11 for, respectively, the confidence limits of 99 % and 99.7 % together with the previous results shown in Fig. 7.

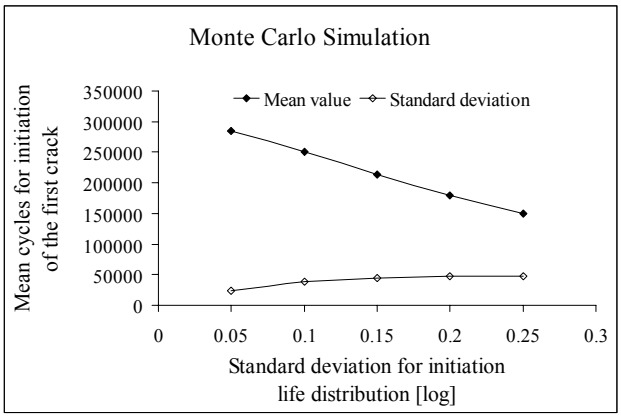

Fig. 9. Effect of the standard deviation on the mean cycles for initiation of the 1st fatigue crack

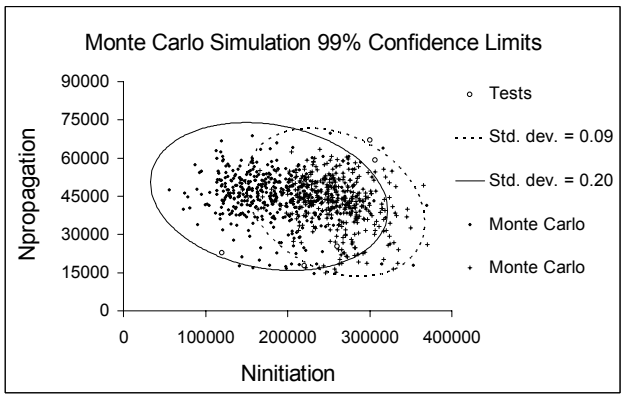

Fig. 10. Monte Carlo simulation results for two different values of standard deviation (Std. dev.)

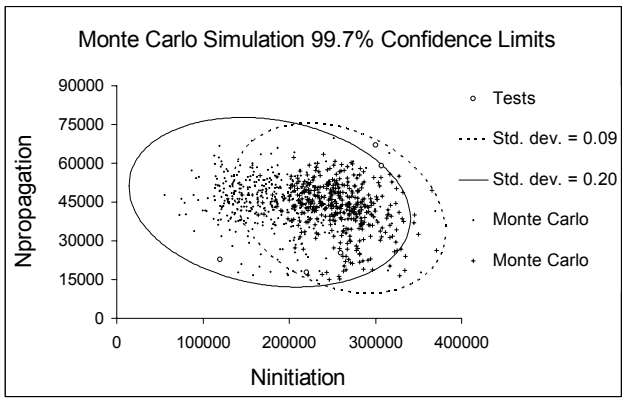

Fig. 11. Monte Carlo simulation results for two different values of standard deviation (Std. dev.)

As observed in section 5.1, Fig. 10 and Fig. 11 show that lives to failure are still dominated by crack initiation, with mean initiation life equal to 258,000 cycles and the mean propagation life equal to 42,500 cycles, i.e., the initiation phase now represents 86 % of the failure process. Total initiation life varies from 1.5×10^5 to 3.7×10^5 cycles, whereas propagation lives are between 1.5×10^4 to 6.4×10^4. If a comparison of these numbers is made with the previous results presented in section 5.1, it can be realized that the mean initiation life has increased by 43 % and the mean propagation life has decreased by only 5.6 %.

From the results shown in Fig. 10 and Fig. 11, the percentage of scenarios which developed 1, 2, 3, 4, 5 and 6 cracks are presented in Fig. 12. From Fig. 12 it can be seen that the percentage of scenarios which developed only one crack decreased to 30 % of the cases, and scenarios containing simultaneous presence of 2 cracks have become the most representative ones. Comparing the results from Fig. 8 and Fig. 12, it can be seen that scenarios containing 5 and 6 cracks have entered the Monte Carlo simulation results.

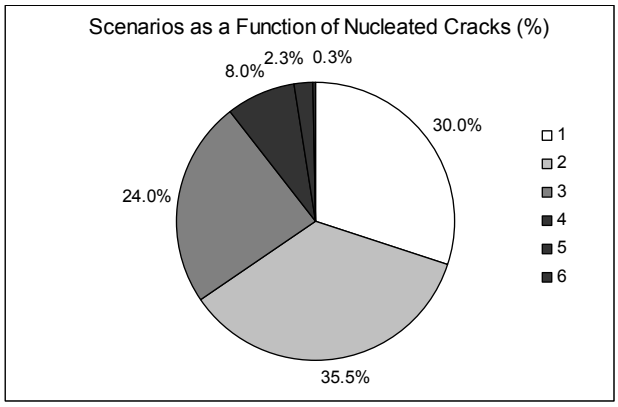

Fig. 12: Percentage of scenarios as a function of nucleated cracks for $\sigma[\log]= 0.09$

From Fig. 10 and Fig. 11, the results demonstrate that a decrease in the standard deviation, for the same mean fatigue life, is proportionally more pronounced in the initiation phase than in the propagation one. The increase of fatigue life in the mean initiation phase value is due to the side effect of the normal distribution, i.e., the normal distribution becomes narrower for decreasing values of standard deviation and therefore the fatigue life for the initiation of the first cracks tend to occur later in time.

From Fig. 8 and Fig. 12, it is noted that a decrease in the standard deviation, for the same mean fatigue life, increases the percentage of MSD-like scenarios. The decrease of the mean propagation life observed in Fig. 10 and Fig. 11 is due to the increase in crack density per scenario. As the presence of cracks increase, the mean time to crack propagation tend to diminish because of an increase in crack interaction effects leading to bigger crack propagation rates.

6 Discussion

Concerning the probabilistic MSD assessment model proposed in this work, from Fig. 7 it can be seen that the 6 experimental test points [20] demonstrate a spread comparable to the 400 Monte Carlo simulation results in both Ninitiation and Npropagation axis, but most noticeably in Npropagation axis. This observation is found in the majority of previous comparisons of Monte Carlo simulation and experimental MSD data in the literature, and suggests that there are causes of scatter in propagation which could be improved in the model. For instance, Santgerma [2] has analysed the same lap joint presented in Fig. 3, without considering either probabilistic crack growth or continuing damage assumption but using damage accumulation calculation for crack re-initiation; and his work gives a similar scatter band on the Npropagation axis to the one presented here.

From Fig. 11 it can be noted that for the same mean fatigue life for initiation of fatigue cracks, and within a possible range of standard deviation values associated with this life, the spread in life for the crack initiation axis is increased up to a point where all the experimental test points are completely enclosed within the two different 99.7 % confidence boundaries. These results suggest that instead of adopting a fixed value for the standard deviation utilized in Monte Carlo simulations, a possible combination of two different values can be employed in order to generate a third confidence region which is formed out of the two previous ones. This procedure for MSD assessment is not proposed in the literature so far, although it is physically possible to occur due to the fact that different standard deviation values can be employed for the same mean time to crack initiation.

Regarding MSD assessment models in general, one of the main reasons for them is the establishment of the Inspection Starting Point

(ISP) and the Structural Modification Point (SMP), used to define the monitoring period. The ISP is the time in life of the structure when special inspection procedures are started to prevent MSD threat; and the SMP is the point beyond which the structure may not be operated without further evaluation. In order to establish the ISP and the SMP, the mean fatigue life to failure (Nf,mean) must be determined. Starting with the results shown in Fig. 7, the value of Nf,mean is given by Nf,mean = Ninit,mean + Nprop,mean = 222,000 cycles, where Ninit,mean and Nprop,mean are respectively, the mean values for crack initiation and crack propagation lives given by the Monte Carlo simulation results. The ISP and the SMP are calculated by dividing Nf,mean by typical factors of 3 and 2 respectively [1]. For these numbers and for the lap joint configuration analysed in this work, the ISP and the SMP values are respectively, 74,000 cycles and 111,000 cycles. Repeat inspection intervals (I_{WFD}) are given by 5,200 cycles (see Appendix I). These numbers are typical of those published in previous studies for flat lap joint configurations such as the one illustrated in Fig. 3.

If the same procedure is used to calculate the ISP, the SMP and the I_{WFD} for the results shown in Fig. 11, regarding the 99.7 % confidence region related to σ[log] equal to 0.09 only, it is found that ISP = 100,000 cycles, SMP = 150,000 cycles and I_{WFD} = 4,500 cycles (based on F_{WFD} = 11). If these values are compared to the ones obtained from the results shown in Fig. 7, it can be realized that both the ISP and the SMP have been increased by 35 % and the I_{WFD} has been decreased by 14 %. The main cause to the increase in the ISP and the SMP is attributed to the mean fatigue life for crack initiation; while the decrease of the I_{WFD} is basically related to the mean fatigue for crack propagation. The variation on these parameters is exclusively related to changes in the standard deviation values. If a mean value for establishment of the ISP, the SMP and the I_{WFD} is considered from both Monte Carlo simulation results shown in Fig. 11, these values would be respectively, 87,000 cycles, 130,500 cycles and 4,850 cycles.

The approximations and assumptions inherent in the current models, some of which are discussed above, suggest that we cannot yet regard the factors 2 and 3 used in the derivations as fixed. It may be that distributions of real test data gathered on large numbers of aircraft would have distributions for which use of the above factors would not result in an acceptably low probability of occurrence of MSD. Fatigue crack initiation input data used in current MSD models commonly come from small flat lap joint specimens manufactured using aircraft standards [26], whereas the ideal situation would be obtaining such input data from a series of full-scale fatigue tests, which is economically prohibitive. As a direct consequence of this issue, MSD models can be describing the MSD behaviour of flat lap joints and not real aircraft structures. Real aircraft lap joints are subjected to bi-axial loads such as circumferential and axial stresses caused by pressurization, bending and torsion caused by aerodynamic loads and landing, not to mention environmental effects that can lead to corrosion. Is his work Okada [27] compares the fatigue lives for initiation of 1 mm cracks from flat panel specimens and one-third scale-models of a B-737 fuselage structure subjected to pressurization and bending loads. If the fatigue life for crack initiation obtained from the scale-model specimens is divided by the corresponding value for flat panel specimens, a mean coefficient of 0.42 is obtained. This coefficient means that the fatigue life for crack initiation is reduced by 58 %.

If the same reduction in fatigue life observed in Reference [27] for crack initiation is considered while calculating the mean ISP and SMP for both Monte Carlo simulation results shown in Fig. 11, the new values will be ISP = 45,000 cycles and SMP = 67,500 cycles. Tear down inspections from full-scale fatigue test reported by Piascik [28] and from aging aircraft reported by Sampath [13] have shown the presence of detectable cracks at respectively, 38,333 cycles and 43,400 flights. Considering one pressurization cycle per flight, these numbers are very close to each other; and an

ISP equal to 45,000 cycles seems to be much more appropriate to represent the beginning of a MSD inspection program in real aircraft lap joints than the ones obtained previously using so lonely the simple fatigue crack initiation data from simple flat lap joint specimens.

It has to be highlighted that the mean coefficient of 0.42 derived from Okada [27] experimental work can not yet be taken has fixed. This value was calculated based on two flat lap joint and two scale-model fatigue test specimens, which can not represent the statistical dispersion inherent to a wider number of fatigue tests. Although, Okada [27] results give a clear indication that there are significant differences from both test specimens results as a source of input data for Monte Carlo simulations. Therefore, for some of the reasons and examples described previously, the applicability of current MSD assessment models, based on simple fatigue crack initiation data obtained from flat lap joint specimens, possibly used to describe aircraft MSD behaviour, can be questioned and it seems that further improvement concerning these models is needed.

5 Summary

- A simple model for representing cracked lap joints has been presented and the results were compared to SIF values published in the literature demonstrating good agreement. The derived model was used to perform a geometrical correction factors investigation, and the results demonstrated that crack interaction effects can take place for cracks positioned more than one pitch distance from each other.
- A probabilistic model for prediction of MSD onset considering both fatigue crack initiation and crack propagation as random variables has been presented.
- The dual boundary elements method has been successfully coupled with Monte Carlo simulation in order to derive a simple approach for probabilistic crack growth assessment of MSD in a riveted lap splice joint.
- The Monte Carlo simulation results, from the probabilistic MSD model presented, were able to enclose both fatigue crack initiation and fatigue crack propagation scatter bands when compared to experimental work from the literature for flat lap joint specimens, demonstrating the effectiveness of the model.
- Possible different standard deviation values for the same range of mean fatigue lives for crack initiation suggest that a combined use of two different Monte Carlo simulation sets should be proposed to represent the initiation phase. The combined Monte Carlo sets proposed demonstrated improvement in the scatter of the MSD assessment model, so that all experimental test points could be enclosed within the sets.
- As reported in the literature, good part of the cracked scenarios generated by Monte Carlo simulation was mono-crack cases. The percentage of mono-crack scenarios is diminished by a decrease in the standard deviation value. Therefore more scenarios resembling MSD-like situations are generated and the mean time to crack propagation is diminished.
- The decrease of the standard deviation value increases the ISP and the SMP values, while the inspection interval is decreased. The mean time to crack initiation demonstrated to be the most important cause of change in the ISP and the SMP values, while changes observed to the inspection interval were basically related to the mean time to crack propagation.
- An example was given where the use of fatigue crack initiation data, obtained from simple flat lap joint specimens, could possibly not represent curved lap joint structures such as the ones in real aircraft.

6 Acknowledgments

The authors would like to express their appreciation to Dr. Nelson Krahenbuhl Salgado (EMBRAER) for his help on the dual boundary element method technique, the Brazilian Air Force (FAB) and the Civil Aviation Authority (CAA) from the U.K. for sponsoring this work.

References

[1] AAWG. Recommendations for Regulatory Action to Prevent Widespread Fatigue Damage in the Commercial Airplane Fleet. *A Report of the Airworthiness Assurance Working Group (AAWG) for the Aviation Rulemaking Advisory Committee Transport Aircraft and Engine Issues*, 1999.

[2] Santgerma A. Developpement d'Une Methodologie de Prevision du Comportement des Strutures d'Avions Civils en Presence de Dommages Multiples de Fatigue. *Doctorate Thesis*, Department of Mechanical Engineering, Toulouse, 1997.

[3] Proppe C. Probabilistic Analysis of Multi-Site Damage in Aircraft Fuselages. *Computational Mechanics*, Vol. 30, pp. 323-329, 2003.

[4] Aliabadi M H and Rooke D P. *Numerical Fracture Mechanics*. Computational Mechanics Publications, Southampton and Kluwer Academic Publishers, Dordrecht, The Netherlands, 1991.

[5] Kebir A, Roelandt J M and Gaudin J. Monte-Carlo Simulations of Life Expectancy Using the Dual Boundary Element Method. *Engineering Fracture Mechanics*, Vol. 68, pp. 1371-1384, 2001.

[6] ESDU. The Compounding Method of Estimating Stress Intensity Factors for Cracks in Complex Configurations Using Solutions from Simple Configurations. *ESDU 78036*, 1978.

[7] Salgado N K and Aliabadi M H. Boundary Element Analysis of Fatigue Crack Propagation in Stiffened Panels. *Journal of Aircraft*, Vol. 35, No. 1, pp. 122-130, 1998.

[8] Salgado N K and Aliabadi M H. The Analysis of Mechanically Fastened Repairs and Lap Joints. *Fatigue Fract. Engng. Struct.*, Vol. 20, No. 4, pp. 583-593, 1997.

[9] Cope D A and Lacy T E. Stress Intensity Determination in Lap Joints with Mechanical Fasteners. *41st AIAA/ASME/ASCE/AHS/ASC Structures*, Structural Dynamics and Materials Conference and Exhibit, Atlanta, GA, pp. 274-283, 2000.

[10] Salgado N K. *Damage Tolerance Design System DTD Computer Code – V. 5.0*. Empresa Brasileira de Aeronautica, S. J. Campos – S. P., Brazil, 1999.

[11] Garcia A N and Irving PE. A Study of Geometrical Correction Factors in a MSD Scenario. *Report CAA/W30637E/57*, SIMS, Cranfield University, 2003.

[12] Horst P and Schmidt H-J. A Concept for the Evaluation of MSD Based on Probabilistic Assumptions. *AGARD SMP Specialists Meeting on Widespread Fatigue Damage in Military Aircraft*, Rotterdam, CP-568, pp. 6.1-6.12, 1995.

[13] Sampath S G, Tong P, Arin K, Jeong D Y, Greif R, Brewer J C and Bobo S N. Current DOT research on the Effect of Multiple Site Damage on Structural Integrity. *International Conference on Aging Aircraft and Structural Airworthiness*, NASA Langley Research Center, pp. 111-157, 1992.

[14] Steadman D, Carter A, Ramakrishnan R. Characterisation of MSD in an In-Service Fuselage Lap Joint. *The Third Joint of DoD/FAA/NASA Conference on Aging Aircraft*, 1999.

[15] Tanaka K. Fatigue Crack Propagation from a Crack Inclined to the Cyclic Tensile Axis. *Engineering Fracture Mechanics*, Vol. 6, pp. 493-507, 1974.

[16] Swift T. Damage Tolerance Capacity. *Fatigue of Aircraft Materials-Proceedings of the Specialists' Conference, Dedicated to the 65th Birthday of J. Schijve*, Delft University, pp. 351-387, 1992.

[17] USAF. Airplane Damage Tolerance Requirements, *Military Specification MIL-A-83444*, 1974.

[18] Xing J and Hong Y J. A Maximum Likelihood Method for Estimates of the Statistics of the Crack Growth Behaviour. *International Journal of Pressure Vessels and Piping,* Vol. 76, pp. 641-646, 1999.

[19] Virkler D A, Hillberry B M and Goal P K. The Statistical Nature of Fatigue Crack Propagation. *Journal of Engineering Materials and Technology*, Vol. 101, pp. 148-153, 1979.

[20] Foulquier J. Fatigue Tests on Simple Lap Joint Specimens, *Report SMAAC TR-3.2-04-1.3/AS*, 1997.

[21] Press W H, Teukolsky S A, Vetterling W T and Flannery B P. *Numerical Recipes in C – The Art of Scientific Computing*. Second Edition, Cambridge University Press , 1992.

[22] Arnold B and Shavelle R M. Joint Confidence Sets for the Mean and Variance of a Normal Distribution. *The American Statistician*, Vol. 52, No. 2, 1998.

[23] Santgerma A, Jean-Yves B and Bruno R. An Example of Widespread Fatigue Damage Assessment in A300 Susceptible Structure. *The Fourth Joint DoD/FAA/NASA Conference on Aging Aircraft*, St. Louis, Missouri, pp. 1-7, 2000.

[24] Meyer E S, Fields S S and Reid P A. Projecting Aircraft Reliability. *Fifth Joint NASA/FAA/DoD Conference on Aging Aircraft*, Orlando, Florida, pp. 1-12, 2001.

[25] Swift T. Repairs to Damage Tolerant Aircraft. *Structural Integrity of Aging Airplanes*, Spring-Verlag Series in Computational Mechanics, Berlin, pp. 433-483, 1991.

[26] Balzano M, Beaufils J-Y and Santgerma A. An Engineering Approach to the Assessment of

Widespread Fatigue Damage in Aircraft Structures. *The Second Joint NAS/FAA/DoD Conference on Aging Aircraft*, Virginia, pp. 124-131, 1998.

[27] Okada T, Terada H and Dybskiy P. Fatigue Behaviour of Lap Joint of Fuselage Model Structure. *Fifth Joint NASA/FAA/DoD Conference on Aging Aircraft*, Orlando, Florida, 2001.

[28] Piascik R S and Willard S A. The Characteristics of Fatigue Damage in Fuselage Riveted Lap Splice Joint, *NASA TP-97-206257*.

Appendix I

Repeat inspection intervals (I_{WFD}) are established based on time from a detectable crack size initiation up to the SMP, divided by a factor (F_{WFD}). Considering the chosen initial crack size value of 1.5 mm as the detectable crack length, the total Inspection Period (IP) is defined as the number of cycles between the ISP and the SMP, i.e., equal to 37,000 cycles. From the 99.7 % confidence limits of Fig. 8, it can be noticed that the smallest time to crack propagation ($TTCP_{MIN}$) up to failure is 12,000 cycles. According to traditional damage tolerance analysis, if $TTCP_{MIN}$ is divided by a safety factor of 2 it will lead to an inspection period of 6,000 cycles. Dividing the IP by 6,000cycles, a factor F_{WFD} = 6.2 is obtained and, consequently, a factor of 7 is more likely to be employed. Therefore, the repeat inspection intervals can be defined as I_{WFD} = IP/F_{WFD} = 5,285 cycles which can be approximated to I_{WFD} = 5,200 cycles.